

# THE PREDICTION OF HYBRID II MANIKIN HEAD-NECK KINEMATICS AND DYNAMICS

JACQUELINE PAVER  
BARRON FISHBURNE

Biomedical Engineering Department  
Duke University  
Durham, N.C. 27706

---

**ABSTRACT** *This paper presents results of an ongoing research program to develop data sets for computer models which accurately predict the head-neck kinematics and dynamics of existing dummies in crash environments. In this study, a data set of the Hybrid II manikin head neck system was developed for the Armstrong Aeromedical Research Laboratory (AAMRL) Articulated Total Body (ATB) Model. The Part 572 Head-Neck Pendulum Compliance Test of the Code of Federal Regulations (CFR), was simulated to validate this data set. Parametric studies were conducted to assess the effects of variations in neck joint characteristics upon the predicted head-neck responses. The final data set predicted head rotation and chordal displacement data which complied with Part 572 specifications. The predicted peak head accelerations were slightly higher than that specified by Part 572.*

**INTRODUCTION** A variety of mathematical models have been developed to predict human biodynamic responses and injury potential in impact environments. In previous studies <sup>1,2</sup>, data sets of the Hybrid II and Hybrid III manikin head-neck structures were developed for the AAMRL Head-Spine Model. The CFR Part 572 and Amended Part 572 Head-Neck Pendulum Compliance Tests <sup>3</sup> were simulated to validate these data sets. In this study, the goal was to develop and validate an ATB Model data set which accurately predicts the mechanical behavior of the Hybrid II manikin head-neck structure. The CFR Part 572 Head-Neck Pendulum Compliance Test was simulated to validate this data set. Parametric studies were conducted to assess the effects of variations in neck joint characteristics upon the predicted head-neck responses.

Hopefully, the information generated by this study will serve as one step toward improving the head and neck injury prediction potential of the ATB model. In particular, the proposed Hybrid II data set will be useful to researchers modeling experiments with this dummy. Ideally, these experiments

and computer simulations will help us understand the responses of humans in similar crash environments. The ATB data set development and parametric studies will also serve as a preliminary effort toward the development and validation of human data sets with accurate neck descriptions. The human data sets will be based upon the results of viscoelastic studies of the biomechanical properties of human cadaver spines.

**BACKGROUND** The mathematical model selected for this study was a whole-body gross-motion simulator model. The ATB Model, which is a modified version of the Calspan Crash Victim Simulator (CVS) Model <sup>4,5</sup>, accommodates several Air Force applications such as encumbrance effects on crew-man performance, vibration loading, and ejection from disabled aircraft. The equations of motion and constraint are formulated from Euler's rigid body equations of motion with Lagrange-type constraints. These equations are solved using a Vector Exponential Integrator and quaternions. In most applications, the crash victim is represented by fifteen segments and fourteen joints; the neck joints are typically ball-and-socket types.

The Hybrid II manikin head-neck system was chosen as the specimen for this study. The head is a hollow two-piece aluminum casting instrumented with accelerometers mounted at its center-of-gravity (cg). Both the skull and rear cap are covered with a rubber skin. The neck is a right circular cylinder constructed of butyl rubber elastomer. It is solid, except for a small hole through the middle. Aluminum plates are molded into each end to facilitate head-neck and head-thorax attachment.

The Hybrid II head-neck calibration test and performance requirements are described in the Code of Federal Regulations, Title 49, Part 572. The head-neck pendulum test (see Figure 1) consists of a pendulum drop. At the bottom of the pendulum's swing, the arm impacts a block of honeycomb. The head-neck system, which is mounted to the end of the pendulum, does not undergo any impact. Part 572 specifies an impact velocity and near square-wave acceleration pulse at the pendulum strike plate (i.e., a range for the average deceleration level above 20g's and minimums for the slopes of the deceleration curve between 5 and 20g's). Only a neck flexion test is required. There are three ways that the head-neck response is specified: (1) head rotation vs. time; (2) chordal displacement of the head cg vs. time; and (3) peak head acceleration and average head acceleration above 20 g's. The chordal displacement at time  $t$  is defined in Figure 2; it is the straight line distance between (1) the position of the head cg relative to the pendulum arm at time zero (the dashed lines); and (2) the position of the head cg relative to the pendulum arm at time  $t$  (the solid lines).

**DATA SET DEVELOPMENT** An ATB data set was developed which accurately predicts the mechanical behavior of the Hybrid II head-neck system. The CFR Part 572 head-neck pendulum compliance test was simulated to validate this data set.

The ATB data set consisted of three segments (the pendulum, head, and neck segments) and three joints (the head-neck of HN, neck-pendulum or NP, and pendulum-vehicle or PV joints). Ball-

and-socket joints were defined between the head and neck and between the neck and pendulum. A pin joint was defined between the pendulum and the vehicle. The geometric and inertial properties of the segments and pendulum-vehicle joint characteristics were abstracted from operational data sets at AAMRL or estimated from the literature 3-7. The neck joint characteristics used initially were estimated from CVS manuals, operational data sets at AAMRL, Part 572, and static test data 4-7. The honeycomb was defined as a contact plane. The specified acceleration-time history was achieved by defining a plane-ellipsoid contact between the pendulum and honeycomb and force-deflection characteristics for that contact. Figure 3 shows a typical acceleration pulse. Simulations were performed of the impact phase, where time zero was the time just prior to pendulum-honeycomb contact. The initial conditions were the positions and velocities of the segments, which were calculated from the Part 572 pendulum strike plate impact velocity.

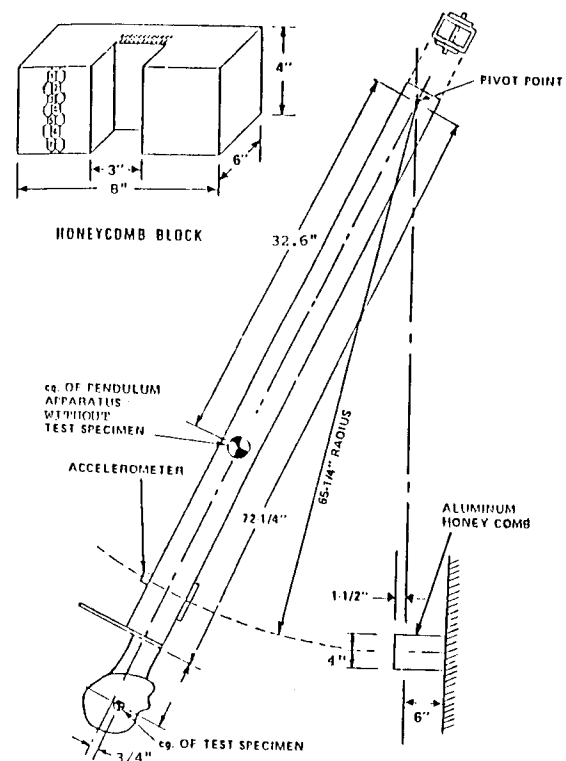
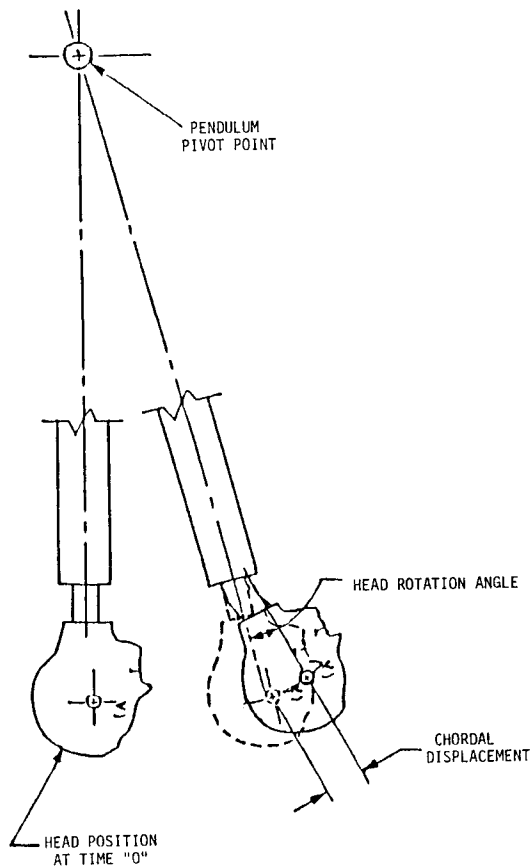
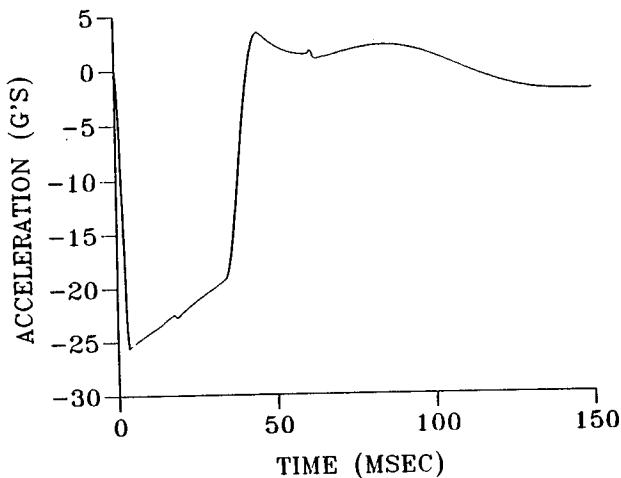


Figure 1 - Pendulum Test Apparatus



**Figure 2 - Response Parameters**



**Figure 3 - Typical Pendulum Strike Plate Acceleration Profile**

The simulations revealed two problems with the initial definition of the pendulum-honeycomb contact. The pendulum was defined as a segment with an attached ellipsoid and the honeycomb was defined as a plane. Plane-ellipsoid contact resulted. Since contact forces are defined in terms of the penetration be-

tween contact surfaces and since the strike plate was located at a distance almost equal to the major axis length of the pendulum ellipsoid, contact was not observed at the right point in space if the dimensions of the pendulum and honeycomb were defined correctly. Both the amount of penetration and the contact time were low. This problem was eliminated by shifting the contact ellipsoid attached to the pendulum so that its center coincided with the center of the strike plate. The second problem related to the contact algorithm, which assumes that no contact occurs and hence no forces are generated after full penetration of the pendulum into the honeycomb. Since this algorithm is not valid for this simulation, the pendulum thickness was increased with no change in its inertial properties. For realistic graphics, the pendulum ellipsoid was removed from the plots and replaced by a rectangular segment in the VIEW program input file. Figure 4 shows the VIEW program output.

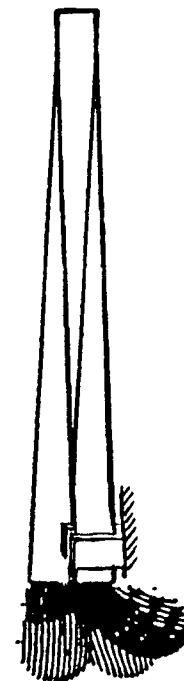


**Figure 4 - VIEW Program Output**

The responses of the model did not comply with the Part 572 performance requirements using the initial data set. The data set was tuned to make the ATB head-neck responses comply with Part 572. Since the geometric and inertial

properties of the Hybrid II head and neck are well documented, these constants remained fixed; they were not used to tune the data set. The values used for the joint characteristics of the neck, however, are not well documented. Parametric studies were conducted to assess the effects of variations in neck joint characteristics upon the predicted head-neck responses. Since the neck joint was modeled as a ball-and-socket type, the relevant joint characteristics are: (1) flexural linear, quadratic, and cubic spring coefficients, energy dissipation coefficient, and joint stop; (2) viscous coefficient; (3) coulomb friction coefficient; and (4) joint lock-unlock conditions. By varying these neck properties in a systematic manner, optimization of the model response with the specifications was possible.

**SIMULATION RESULTS** Figures 5-16 show the results of the parameter tuning process. Plots labeled 572 illustrate the final data set results. The final data set predicted head rotation and chordal displacement data which complied with Part 572 specifications. The predicted peak head accelerations were slightly higher than that specified by Part 572. Plots labeled H illustrate the predicted responses when a higher value is used for the selected parameter. Plots labeled L illustrate the predicted responses when a lower value is used for the selected parameter.

It was found that an increase in the HN linear flexural spring coefficient decreased the amplitude and period of the head rotation but decreased the amplitude and increased the period of the chordal displacement (Figures 5-6). The effects of changes in the HN viscous and HN coulomb friction coefficients were similar (Figures 7-10). An increase in the parameter above the 572 value decreased the amplitude of the head rotation with little change in the chordal displacement. A decrease in the parameter below the 572 value produced little change in the responses. Increasing the NP linear flexural spring coefficient decreased the amplitude and period of both the head rotation and chordal displacement (Figures 11-12). The effects of changes in the NP viscous and NP

coulomb friction coefficients were similar (Figures 13-16). An increase in the parameter decreased the amplitude but increased the period of both the head rotation and chordal displacement. Decreasing the NP joint stop, however, decreased the period of the head rotation and decreased both the amplitude and period of the chordal displacement. Increases in the energy dissipation coefficients with the smaller joint stop angles had little effect on the responses. The effects of changes in the full friction angular velocity and changes in the torsional coefficients over several orders of magnitude were negligible. Finally, increasing the NP linear flexural spring, viscous, or coulomb friction coefficients reduced the predicted head accelerations by approximately 10%. Changes in all other parameters over several orders of magnitude had little effect on the predicted head accelerations.

**Table I - Neck Joint Characteristics**

Parameter	Joint	L	572	H
Linear Flex. Spring Coeff. (in-lb/deg)	HN	7.	35.	3500.
	NP	10.	20.	40.
Joint Stop (deg)	HN	30.	90.	
	NP	45.	90.	
Energy Diss. Coefficient	HN		0.63	1.0
	NP		0.66	1.0
Viscous Coefficient (in-lb-sec/deg)	HN	0.0015	0.15	1.5
	NP	0.0020	0.20	0.4
Coulomb Friction Coeff. (in-lb)	HN	0.5	50.	500.
	NP	0.125	125.	250.
Full Friction Ang. Velocity (deg/sec)	HN	3.	30.	300.
	NP	3.	30.	300.

**SUMMARY AND RECOMMENDATIONS**

A data set of the Hybrid II manikin head-neck system was developed for the ATB Model. The Part 572 Head-Neck Pendulum Compliance Test, of the Code of Federal Regulations, was simulated to validate this data set. Parameterizations were performed to assess the effects of changes in neck joint characteristics upon the model responses.

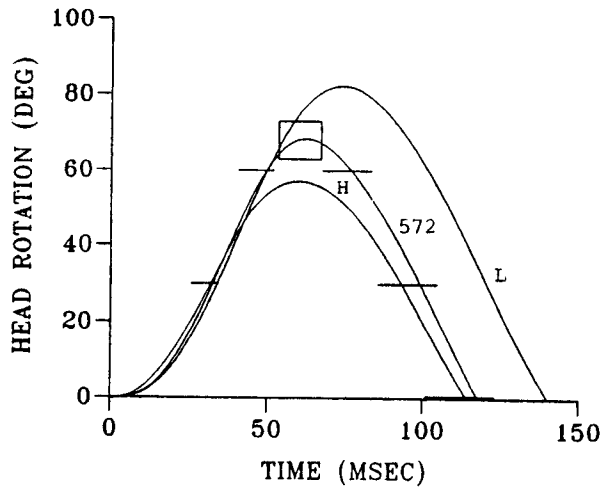


FIGURE 5: EFFECT OF HN LINEAR FLEXURAL SPRING COEFFICIENT VARIATIONS

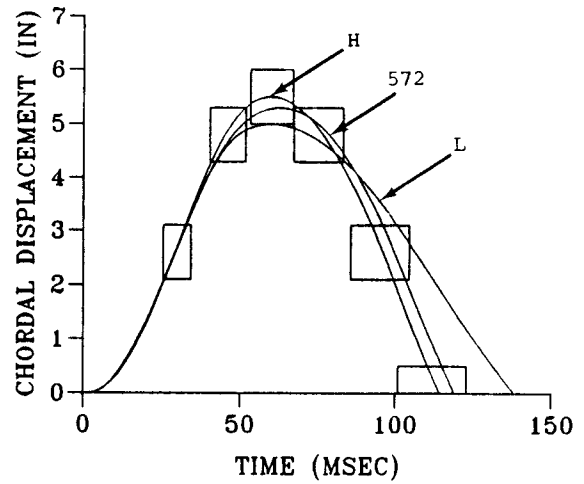


FIGURE 6: EFFECT OF HN LINEAR FLEXURAL SPRING COEFFICIENT VARIATIONS

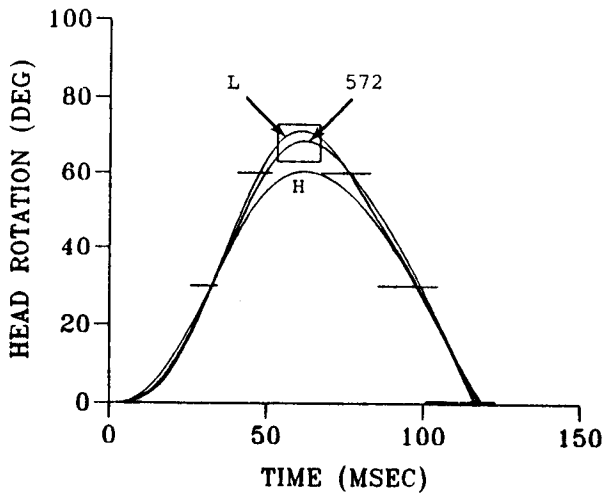


FIGURE 7: EFFECT OF HN VISCOUS COEFFICIENT VARIATIONS

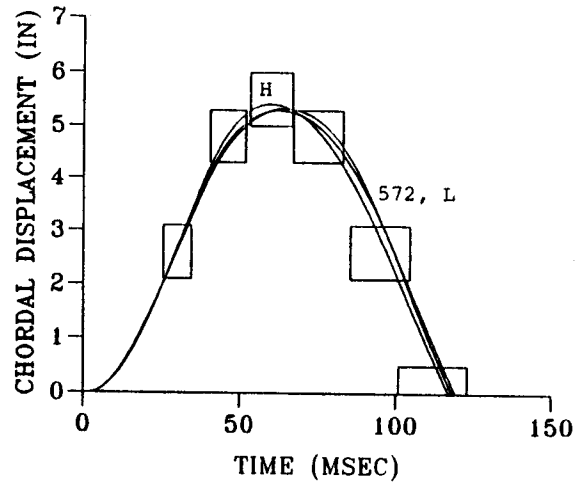


FIGURE 8: EFFECT OF HN VISCOUS COEFFICIENT VARIATIONS

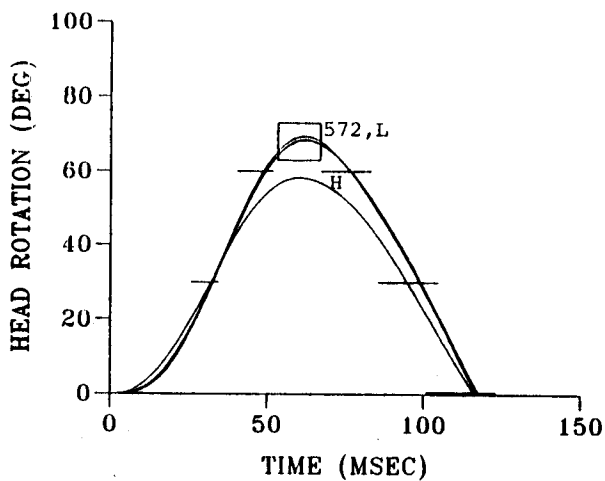


FIGURE 9: EFFECT OF HN COULOMB FRICTION COEFFICIENT VARIATIONS

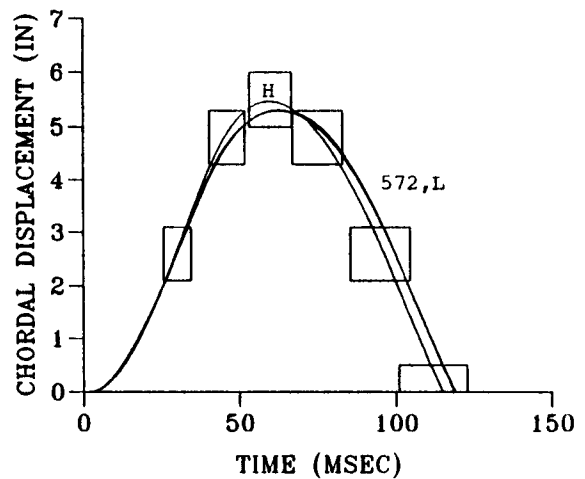


FIGURE 10: EFFECT OF HN COULOMB FRICTION COEFFICIENT VARIATIONS

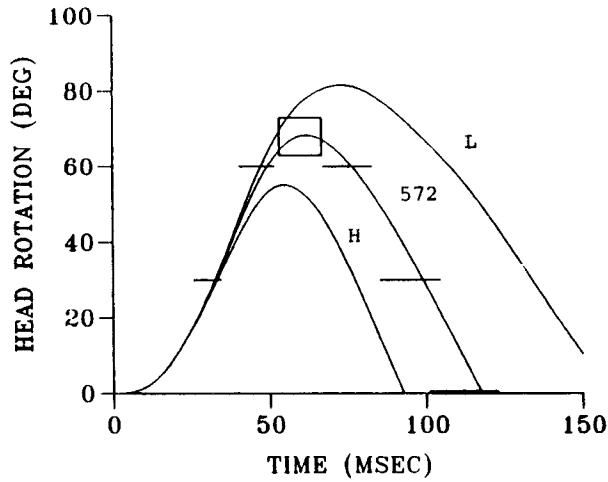


FIGURE 11: EFFECT OF NP LINEAR FLEXURAL SPRING COEFFICIENT VARIATIONS

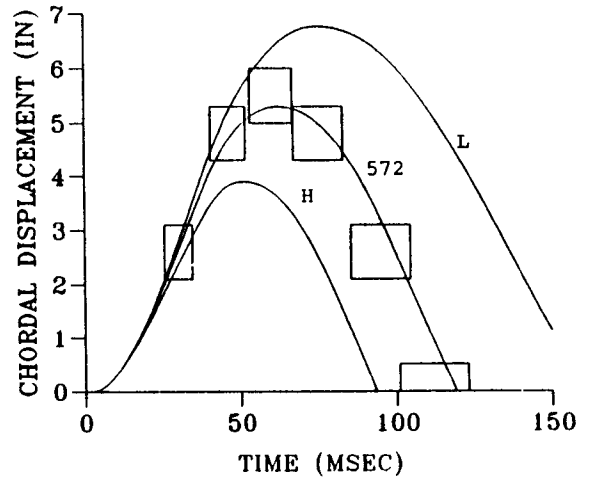


FIGURE 12: EFFECT OF NP LINEAR FLEXURAL SPRING COEFFICIENT VARIATIONS

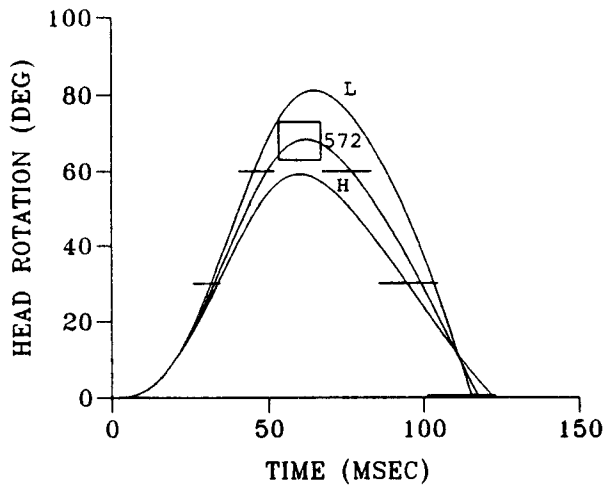


FIGURE 13: EFFECT OF NP VISCOUS COEFFICIENT VARIATIONS

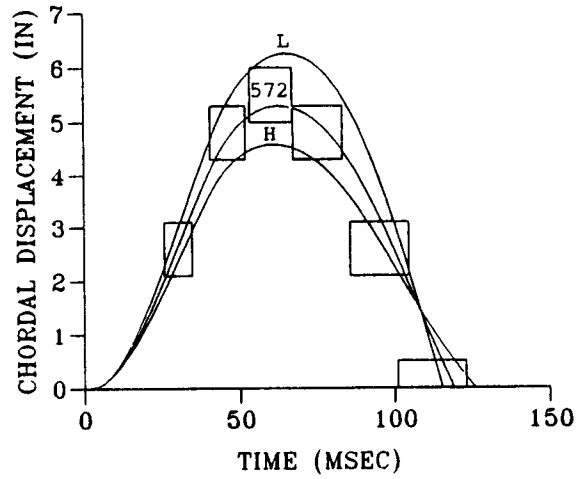


FIGURE 14: EFFECT OF NP VISCOUS COEFFICIENT VARIATIONS

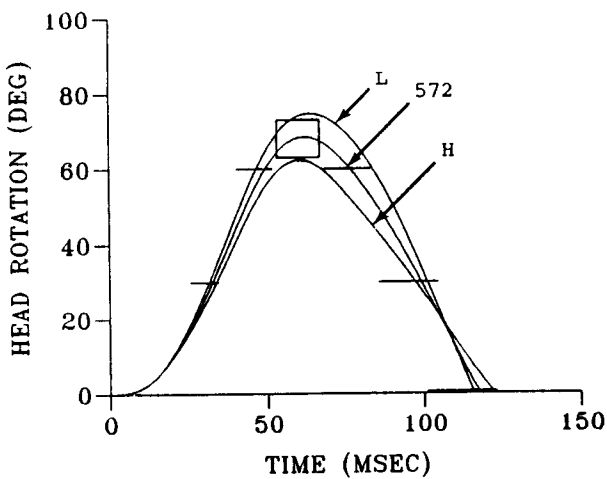


FIGURE 15: EFFECT OF NP COULOMB FRICTION COEFFICIENT VARIATIONS

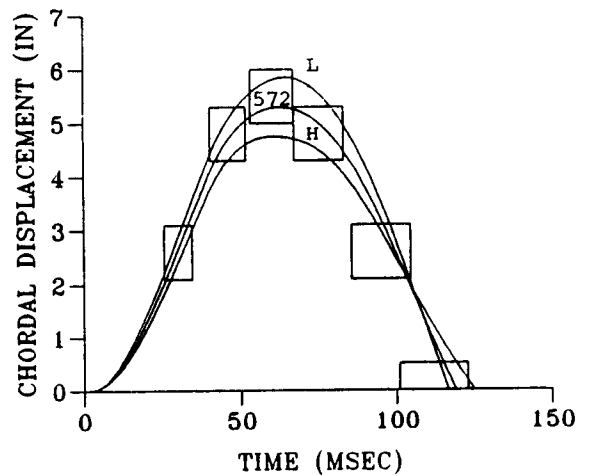


FIGURE 16: EFFECT OF NP COULOMB FRICTION COEFFICIENT VARIATIONS

The following are recommendations for future work: (1) continue tuning the proposed Hybrid II data set by additional validation studies; (2) develop and validate data sets of human and other mechanical head neck systems; and (3) compare dummy responses with human volunteer and cadaver data to assess the biofidelity of these systems.

**ACKNOWLEDGEMENTS** This research was sponsored by the Air Force Office of Scientific Research/AFSC, United States Air Force, under Contract F49620-85-C-0013. The United States Government is authorized to reproduce and distribute reprints for governmental purposes notwithstanding any copyright notation hereon.

#### **REFERENCES**

1. Doherty, B.J.; Paver, J.G.: A Computer Simulation of the Hybrid II Manikin Head-Neck System. Proceedings of the 24th Annual Symposium of the SAFE Association, 1986.
2. Doherty, B.J.; Paver, J.G.: Mathematical Modeling of the Hybrid III Manikin Head-Neck Structure. Proceedings of the International Conference on Mathematical Modeling, 1987.
3. Code of Federal Regulations, Title 49, Part 572 and Amended Part 572.
4. Butler, F.E.; Fleck, J.T.: Validation of the Crash Victim Simulator. Calspan Corporation, DOT Report # DOT-HS-806 279-282, March 1972.
5. Fleck, J.T.; Butler, F.E.; Vogel, S.L.: An Improved Three-Dimensional Computer Simulation of Vehicle Crash Victims. Calspan Corporation. NTIS # PB-241-692-695, April 1975.
6. Hubbard, R.P.; McLeod, D.G.: Geometric, Inertial, and Joint Characteristics of Two Part 572 Dummies for Occupant Modeling. Proceedings of the 21st Stapp Car Crash

Conference, SAE PAPER # 770937, 1977.

7. Miller, J.S.: Performance Evaluation of the GM Hybrid II Anthropometric Test Dummy. NTIS Report # PB224-005, 1973.

#### **BIOGRAPHIES**

Jacqueline Paver is a Research Assistant Professor at Duke University. She received the B.S. degree in Engineering from Harvey Mudd College in 1977 and the M.S. and Ph.D. degrees in Biomedical Engineering from Duke University in 1980 and 1985 respectively. Since 1977, she has worked on a variety of theoretical and experimental projects dealing with the biomechanics of human trauma. Her primary research interest is the biomechanics of head and neck injury and protection.

Barron Fishburne is a first-year medical student at the University of Oklahoma. He received the B. S. degree from Duke University with a double major in Biomedical and Electrical Engineering in 1987. During his senior year, he was responsible for interfacing the ATB and AMRLVIEW programs with available hardware and graphics drivers. He also developed additional post-processing software and performed a variety of accident simulations using the ATB model.